

Heat Capacity of Fish Oil at High Temperatures and Pressures

Z.I. Zaripov, R.R. Nakipov, S.V. Mazanov, A.Kh. Sadykov,
A.R. Gabitova, A.U. Aetov*, F.M. Gumerov

Kazan National Research Technological University, 68 Karl Marx str., Kazan, Russian Federation

Article info

Received:
17 April 2024

Received in revised form:
29 May 2024

Accepted:
16 July 2024

Keywords:

Fish oil
Heat capacity
High temperatures
High pressures

Abstract

This paper reports new results from studies of the isobaric heat capacities of OMEGA-3 “950” fish oil provided by SOLGAR INC (USA) at high temperatures and high pressures. The measurements were carried out on a differential scanning calorimeter (ITs-400) with an automatic data acquisition system in the temperature range from 298.15 to 473.15 K and at pressures from 0.098 to 39.2 MPa. The coverage factor for the 95% confidence level for a two-way coverage interval is assumed to be 2. The expanded measurement uncertainty of heat capacity is estimated to be 2.4%, pressure is estimated to be 0.05% and temperature is estimated to be 15 mK. Experimental data on the fish oil isobaric heat capacity as a function of temperature and pressure are approximated by the correlation equation proposed in the work. At atmospheric pressure, the deviations between those calculated by the correlation equation and the current measured data on isobaric heat capacity are within the range of average absolute deviations (AAD) = 0.22% (standard deviation St. Dev = 0.28% and maximum deviation Max. Dev = 0.39%). Additionally, a comparison was made of the state parameters obtained during the experiment and the literature data at the studied parameters.

1. Introduction

The increase in consumption of hydrocarbon fuels at a high rate of decline in its reserves, tangible environmental consequences from its use, the energy dependence of a significant number of countries without their own reserves of oil, gas and coal, as well as overproduction in agriculture have formed a natural trend towards the search and development of renewable energy sources in based on the processing of biological raw materials [1]. These include biodiesel fuel [2], produced primarily by transesterification of vegetable oils or animal fats (including fish oil) in an alcoholic medium (often methanol or ethanol).

One of the most promising renewable sources of raw materials for biofuel production is microalgae. In terms of energy yield, microalgae are significantly superior to palm and rapeseed oil, usually used for biodiesel production [3,4]. The use of microalgae for fuel production makes it possible to simultaneously solve economic, energy and environmental problems; at the same time, microalgae are a source of such useful substances as Omega-3 (eicosapentaenoic acid), Omega-6 (docosahexaenoic acid), Squalene, etc. Although production biodiesel from them seems promising, technologies for rapid and cost-effective conversion of biodiesel from wet microalgae are still lacking. Various types of extraction are used to extract valuable components from microalgae. The largest amount of Omega-3 and Omega-6 is found in fish oil. At the moment, supercritical fluid extraction with carbon dioxide as an extractant [5–7], carried out at temperatures above 323 K and

*Corresponding author.
E-mail address: aetovalmaz@mail.ru

pressures of 25–35 MPa, is considered the most advanced method for their production [7]. Efficient extraction is characterized by maximum yield of the target component, as well as optimal process parameters in terms of energy consumption. At the stage of mathematical modeling of the extraction process, design and scaling of future technology, the properties of the corresponding thermodynamic systems are required. In particular, the heat capacity of both feedstock and extracts. Analysis of literature sources showed a limited amount of data on the properties of fish oil. Information on the properties of various samples of fish oil from various manufacturers is presented by data on composition, melting points, specific heat capacity and enthalpy at atmospheric pressure [8,9]. S. Sathivel et al. [8] reported the results of studying the melting point, enthalpy and specific heat of catfish visceral fat at different stages of the purification process. In [8], differential scanning calorimetry DSC 2920 (TA Instruments, New Castle, DE, USA) was used to measure the heat capacity and enthalpy of fusion. The heat capacity and enthalpy of fusion of fish oil, both raw and processed, depended on the type of processing. S. Sathivel [9] studied the thermal and transfer properties of unrefined oils from sockeye and pink salmon heads. The degradation and melting temperatures of oils, as well as their heat capacities, were determined. Research [8,9] has established the influence of the composition, type of fish, and processing of raw materials on the heat capacity. Studies were carried out on the transport (thermal conductivity) and thermal properties (coefficient of thermal expansion) of fish oil samples (OMEGA-3 “950”) at pressures above atmospheric [10,11]. Existing calculation methods for determining heat capacity, based on the methods of corresponding states [12–14] and group components [15–17], predict heat capacity values at atmospheric pressure for individual representatives of fatty acids, binary, ternary and multicomponent mixtures, without affecting the influence of pressure.

Based on the above, the main goal of this work is to provide accurate and reliable data on the heat capacity at high pressure (up to 39.2 MPa) and high temperature (from ambient temperature to 473.15

K) ($C_p=f(P,T)$) for a fish oil sample in various thermodynamic calculations. The studied range of temperatures and pressures exceeds the known experimental data, which is the novelty of the work.

2. Materials and methods

OMEGA-3 “950” fish oil sample was provided by SOLGAR INC (USA) ($n_D^{25} = 1.4792$, $\rho_4^{25} = 904.8 \text{ kg/m}^3$). The sample was used without further purification. According to the manufacturer, the sample was obtained by molecular distillation of fish oil from deep-sea fish of the cold seas (anchovy, mackerel, sardine, herring). The sample description is given in Table 1.

Equipment and procedures. Measurements of the fish oil isobaric heat capacity were performed using a differential scanning calorimeter (DSC) (ITS-400) with an automatic data acquisition system (Fig. 1).

The operating principle of a scanning calorimeter is based on the method of monotonic heating of a sample in an adiabatic mode, the fundamentals of which are outlined in the work of Platunov [18]. The essence of the method for measuring the heat capacity of a substance when using the installation (ITS-400) comes down to determining the delay time of the set temperature on the heat meter for the reference and test substance. The sample is heated at such a rate that, within the permissible temperature difference inside the sample, all its layers are heated at each moment of time with almost the same temperature, coinciding with the heating rate b_0 of the base point of the sample. The thermal diagram of the calorimeter is shown in Fig. 2.

A sample of substance 1 is placed in a metal ampoule 2 and heated by a heat flux $Q(T)$ through a heat meter 3. The side surface of the ampoule and the heat meter are surrounded by an adiabatic shell 4. With a stationary thermal field in the heat meter 3, the heat flux $QT(t)$ passing through the heat meter is determined by the formula:

$$Q_T(t) = k_T(t) \cdot \theta_T(t), \quad (1)$$

where $k_T(t)$ – thermal conductivity of heat meter; $\theta_T(t)$ – temperature difference in the working layer.

Table 1. Sample purity information

Chemical name	Provider	Initial purity, %	Final purity, %	Method of analysis
OMEGA-3 “950” (eicosapentaenoic acid (EPA) 53.05% (wt.), docosahexaenoic acid (DHA) 39.79% (wt.), excipients 7.16% (wt.))	SOLGAR INC (USA)	99.0	99.0	Gas-liquid chromatography

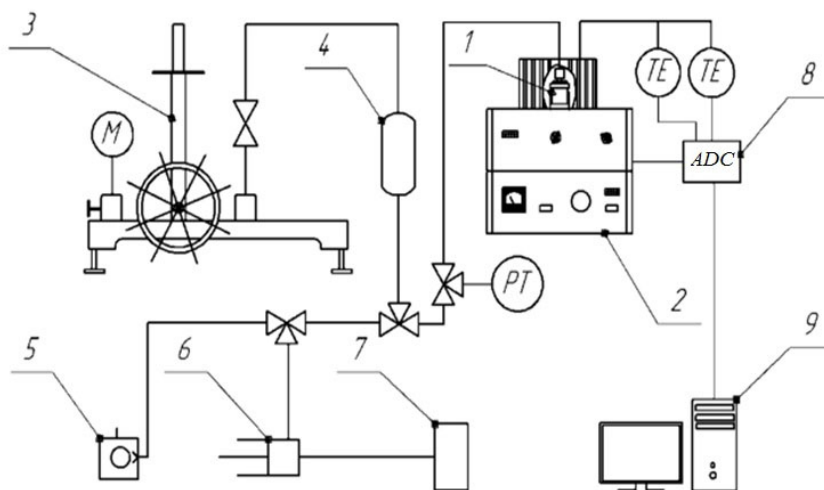


Fig. 1. Schematic diagram of the unit: 1 – measuring cell; 2 – ITS-400 heat capacity meter; 3 – MP-600 deadweight pressure gage tester; 4 – separating bellows assembly; 5 – vacuum pump; 6 – LIQUOPUMP 312/1 fluid-flow pump; 7 – vessel with test substance; 8 – analog-to-digital converter; 9 – personal computer.

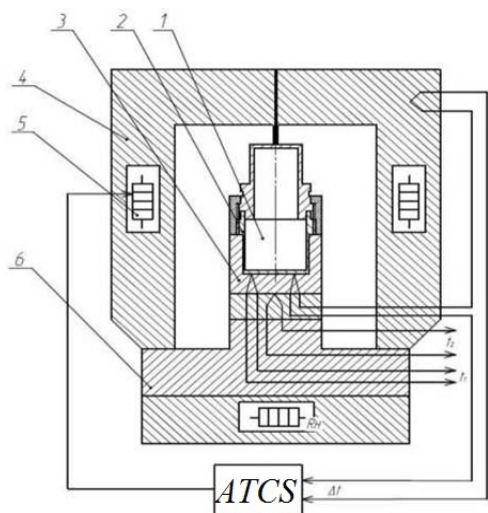


Fig. 2. Thermal diagram of the IT-s-400 device: 1 – test sample; 2 – metal ampoule with lid; 3 – heat meter; 4 – adiabatic shell; 5 – adiabatic heater; 6 – block base; t_1, t_2 – thermocouples. ATCS – automatic temperature control system, R_H calorimetric heater.

The heat balance equation for the ampoule with the sample is written as follows:

$$k_T(t) \cdot \theta_T(t) = C_a(t) \cdot b_a(\tau) + C_0(t) \cdot b_0(\tau) - Q_{dis}(t). \quad (2)$$

Here the indices T, a and 0 refer to the heat meter, ampoule and sample. $C_a(t)$ – heat capacity of the ampoule, $C_0(t)$ – heat capacity of the sample, b_0 – average volumetric heating rate of the sample, $Q_{dis}(t)$ – dissipated heat flux. It must be taken into account, since in real conditions it isn't possible to ensure complete thermal insulation of the ampoule.

If we assume that the magnitude of the dissipated heat flux is proportional to the temperature difference:

$$Q_{dis} = q_{dis} \theta_T(t), \quad (3)$$

then (2) can be represented as

$$K_T(t) \cdot \theta_T(t) = C_a(t) \cdot b_a(\tau) + C_0(t) \cdot b_0(\tau). \quad (4)$$

Here $K_T(t) = k_T + q_{dis}$ and $C_a(t)$ – installation parameters that are functions of temperature only.

For small temperature differences on the heat meter, the equality is well satisfied $\tau_T(t) = \theta_T(t)/b_a(t)$ allowing to record the delay time $\tau_m(t)$ of the ampoule temperature relative to the base of the heat meter. In this case, provided that $b_a(\tau) = b_0(\tau)$, calculation formulas take the following form:

$$K_T(t) \cdot \tau_T(t) = C_a(t) + C_0(t), \quad (5)$$

$$K_T(t) \cdot \tau'_T(t) = C_a(t), \quad (6)$$

$$K_T(t) \cdot \tau''_T(t) = C_a(t) + C''_0(t). \quad (7)$$

Constants of the measuring device $K_T(t)$ и $C_0(t)$ are determined from experiments with an empty cell (index «'») and with a cell filled with a standard liquid (index «''). Here $\tau'_T(t)$ – delay time in an experiment with an empty ampoule, $\tau''_T(t)$ – the corresponding delay time in experiments with a reference liquid, $\tau_T(t)$ – delay time on the heat meter in experiments with the liquid being studied. The solution of Eqs. (5) – (7) has the following form:

$$C_0(t) = C_0''(t) \cdot \frac{\tau_T(t) - \tau_T'(t)}{\tau_T''(t) - \tau_T'(t)} \quad (8)$$

Considering that

$$C_0(t) = c_p(t)m_0, \quad (9)$$

$$C_0''(t) = c_p''(t)m_0'', \quad (10)$$

For the specific isobaric heat capacity of the liquid under study we obtain:

$$C_p(p,t) = c_p''(p_0,t) \cdot \frac{m_0''}{m_0} \cdot \frac{\tau_T(t) - \tau_T'(t)}{\tau_T''(t) - \tau_T'(t)} \quad (11)$$

In Eq. (11) $c_p(p,t)$ and $c_p''(p_0,t)$ – specific isobaric heat capacities of the test and reference liquids, m_0 and m_0'' – respectively, the masses of the test and reference liquids. The calculation expression for determining the isobaric heat capacity in the relative version of the adiabatic dynamic s-calorimeter method is the modified (11) for studies under excess pressure in a cell of constant volume [19–21]:

$$C_p(p,t) = c_p''(p_0,t) \cdot \frac{\rho''}{\rho} \cdot \frac{\tau_T(t) - \tau_T'(t)}{\tau_T''(t) - \tau_T'(t)} \quad (12)$$

where $c_p(p,t)$ and $c_p''(p_0,t)$ – specific isobaric heat capacities of the test and reference liquids at pressure p and atmospheric pressure p_0 and temperature t , J/(kg·K), respectively; ρ and ρ'' – densities of the test and reference liquids at pressure p and atmospheric pressure p_0 and temperature t , kg/m³.

The measuring cell shown in Fig. 3 is first pre-weighed on a VLA-200M analytical balance, then connected to the pipelines, and inserted into an ITS-400 calorimeter. Next, the system is evacuated using an NVR-5DM vacuum pump, allowing the substance being studied to flow from the calibrated flask into the pipelines and measuring cell.

The pressure within the measuring cell is created using a LIQUOPUMP 312/1 fluid-flow pump. Once the desired operating pressure is achieved in the measuring cell, the pump is turned off, and the pressure is maintained by the pressure generation system. The measuring process commences once the ITS-400 measuring unit has cooled to the initial operating temperature. Once the measuring thermocouples, connected to a personal computer via amplifiers and a PCL-811S analog-to-digital converter (ADC), are calibrated, the measuring program begins. The thermocouple interrogation time, measurement duration, and temperature settings are pre-set. During the heating phase, different sections of the mea-

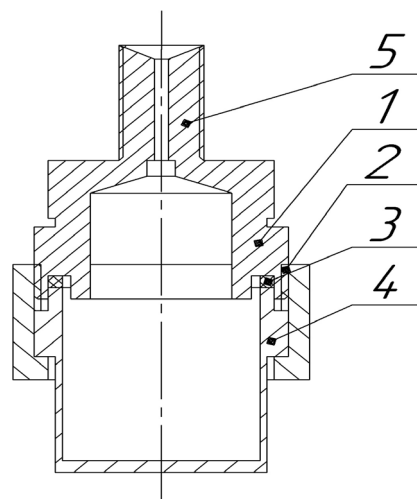


Fig. 3. Measuring cell. 1 – cap; 2 – cap nut; 3 – gasket; 4 – body; 5 – fitting.

suring unit are gradually heated at a constant rate until they reach equilibrium. The measuring thermocouples detect when the temperature mark is surpassed and record the delay time, which is displayed on the PC monitor (Fig. 4). The measuring process concludes upon reaching the specified temperature. From the obtained thermograms, the temperature dependence diagrams of the delay time can be plotted, allowing for the calculation of heat capacity.

The reliability and accuracy of the data on the measured heat capacity of the test sample and the adequacy of the installation are confirmed by measurements of the heat capacity of liquids with well-known and reliable, available experimental data. In order to validate the precision and reliability of the heat capacity data obtained for the sample of OMEGA-3 "950" fish oil, measurements were conducted on reference fluids with known heat capacity values – water [22] and n-heptane [23]. Additionally, experimental heat capacity data for 1-butanol [24] were

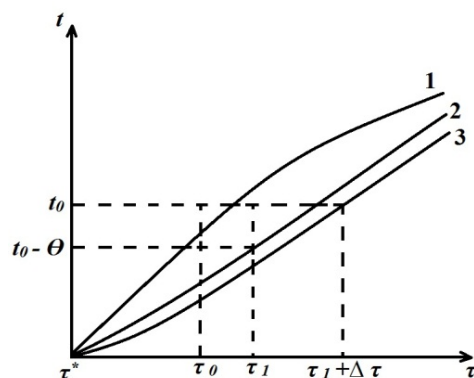


Fig. 4. Time dependences of temperature: 1 – base temperature, 2 – ampoule temperature, 3 – sample temperature, τ^* – moment of heater switching on.

also considered. The results demonstrated a high level of agreement between the test measurements and the reference data $C_p(P, T)$ for water [22], with a deviation of AAD = 0.25% in the temperature range of (333 to 453) K at a pressure of 24.5 MPa. Similarly, the deviations for n-heptane [23] and 1-butanol [24] were within AAD = 0.43% and AAD = 0.88% at pressures of 9.8 MPa and 18.38 MPa, respectively. Dodecane was used as a reference liquid when measuring the heat capacity of a fish oil sample at atmospheric pressure [22]. When measuring the heat capacity of a fish oil sample at pressures above atmospheric pressure, a relative measurement method was used, where the reference substance was the sample itself at atmospheric pressure p_0 .

The small deviations observed are consistent with the experimental uncertainties of the method used. The strong agreement between the present measurements and the reference data for the heat capacity of the liquids verifies the accuracy and reliability of the experimental setup utilized in measuring the heat capacity data for OMEGA-3 "950" fish oil.

3. Results and discussion

The measured values of the fish oil isobaric heat capacity depending on temperature and pressure in the temperature range from 298.15 to 473.15 K and at pressures from 0.098 to 39.2 MPa are presented in Figs. 5 and 6.

Experimental data on the fish oil isobaric heat capacity as a function of temperature and pressure are approximated by an Eq. (13):

$$C_p(P, T) = a_0 + a_1T + a_2P + a_3PT + a_4T^2 + a_5P^2, \quad (13)$$

where, $C_p(P, T)$ is isobaric heat capacity at given P and T, kJ/(kg·K); a_i ($i = 0.5$) are fitting parameters (5 experiment repetitions). The optimal values of the obtained fitting parameters along with the statistics of deviations are given in Table 2.

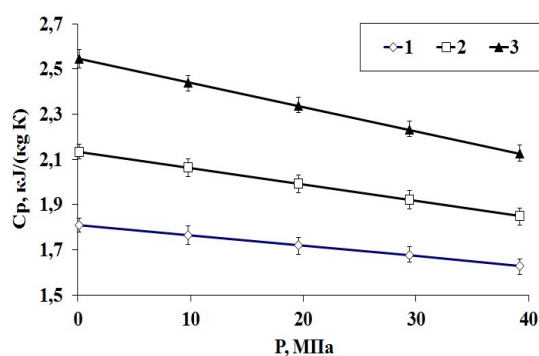


Fig. 5. Dependence of the fish oil isobaric heat capacity on pressure P, MPa: 1 – 298,15 K; 2 – 373,15 K; 3 – 473,15 K.

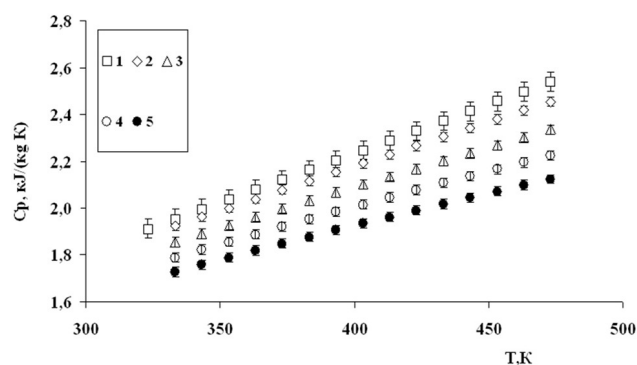


Fig. 6. Dependence of the fish oil isobaric heat capacity on temperature at pressure P, MPa: 1 – 0.098; 2 – 9.8; 3 – 19.6; 4 – 29.4; 5 – 39.2.

Table 2. Polynomial coefficients a_j for calculating the fish oil heat capacity in the temperature range from 298.15 to 473.15 K and pressures from 0.098 to 39.2 MPa

Polynomial coefficients a_j	
a_0 , kJ/(kg·K)	0.7717
a_1 , kJ/(kg·K ²)	$3.313 \cdot 10^{-3}$
a_2 , kJ/(kg·K·MPa)	$-3.718 \cdot 10^{-4}$
a_3 , kJ/(kg·K ² ·MPa)	$-1.74 \cdot 10^{-5}$
a_4 , kJ/(kg·K ³)	$1.095 \cdot 10^{-6}$
a_5 , kJ/(kg·K·MPa ²)	–
St. Dev, %	0.28
AAD%	0.22

As can be seen from the Table 2, the correlation Eq. (13) represents the current data on the fish oil heat capacity within the limits of their experimental

uncertainty $\left(AAD = \frac{100}{N} \sum_{i=1}^N \frac{|Cp_{exp}^i - Cp_{cal}^i|}{Cp_{exp}^i} = 0.22\% \right)$, including

high pressure C_p values. At atmospheric pressure, the deviations between those calculated by the correlation Eq. (13) and the current measured data $C_p(P, T)$ are within the limits of AAD = 0.22% (standard deviation St. Dev = 0.28% and $MAAD = \text{MAX} \left[\frac{|Cp_{exp}^i - Cp_{cal}^i|}{Cp_{exp}^i} \right] = 0.39\%$).

4. Comparison with literature data

Correlation Eq. (13) was used to compare the present heat capacity data for fish oil with published experimental data [8] and with calculations using the method of corresponding states [12–14], and group components [15–17]. When calculating using methods [12–17], knowledge of the composition and critical parameters of the substance is required.

The fish oil sample studied is a mixture of two unsaturated fatty acids (EPA + DHA) in a ratio of 0.609:0.391. Heat capacity calculations using methods [12,14–17] were carried out for mixtures of these acids.

Calculation of the heat capacity C_p of fish oil at atmospheric pressure is considered using the equations:

- Bondi [12]:

$$\frac{C_p - C_p^0}{R} = 2,56 + 0,436(1 - \tau)^{-1} + \omega \left[2,91 + \frac{4,28(1 - \tau)^{1/3}}{\tau} + 0,296(1 - \tau)^{-1} \right]; \quad (14)$$

where the values of the Pitzer acentricity factor (ω) are calculated according to the additivity rule for group composition [12]. - Filippov [14]:

$$C_p - C_p^0 = 20 + 3,9 \frac{\tau^2}{1 - \tau} + \left(74 - \frac{24,4}{\tau} + \frac{12,5}{\tau^2} \right) \cdot \lg \left(\frac{4}{A} \right), \quad (15)$$

Filippov's criterion A is calculated based on the increments given in [14];

- Ruzicka [15]:

$$\frac{C}{R} = \sum_{i=1}^k n_i \cdot \Delta c_i, \quad (16)$$

where n_i is the number of group bonds of type i ; Δc_i is the heat capacity per group bond of type i ; k is the total number of group bonds in the molecule. The values of the group component of the heat capacity are determined by the formula $\Delta c_{i,k} = a + b(T/100) + d(T/100)^2$, where a , b , d are temperature dependence constants;

- Ceriani [16]:

$$C_{p_i}^I = \sum_k N_k \cdot (A_k + B_k \cdot T), \quad (17)$$

where N_k is the number of groups k in the molecule; A_k and B_k are parameters obtained from the regression of the experimental data; k represents the groups of component i ;

- Zhu [17]:

$$C_p = 1.794 + 2.64 \cdot 10^{-3} \cdot T + 1.04 \cdot 10^{-2} \cdot C - 6.6 \cdot 10^{-2} \cdot U, \quad (18)$$

where T is the temperature, °C; C is the average carbon number of all the fatty acids in the lipid; U is the average number of double bonds for all the fatty acids in the lipid.

Comparison of data from [8] with the calculation using correlation Eq. (13) extrapolated to a temperature of 293 K and atmospheric pressure showed the following: for example, the specific heat capacity of raw fish oil differs from the data according to Eq. (13) by 8%, degummed by – 6.7%, neutralized by – 7.27%, bleached by – 4% and deodorized somatic fat by 0.36%, respectively. At the same time, the heat capacity of fat varied depending on the type of processing from 1.69 to 1.97 kJ/(kg·K). Significant deviations in the heat capacity data [8] are caused by the

presence of impurities in them, such as phospholipids, free fatty acids, aldehydes, ketones, water and pigments. The heat capacity of deodorized somatic fat ($C_p = 1.837$ kJ/(kg·K)) according to [8] (the unsaturated fatty acids content is about 68%) is close to the calculated heat capacity of Eq. (13).

Figure 7 shows the calculated according to [12,14–17] and experimental data on the heat capacity of the studied sample of fish oil at atmospheric pressure. As can be seen from Fig. 7, the calculated C_p data using the method of [14] are systematically higher than current measurements by an average of 6.36%. Figure 8 shows the percentage deviations (deviation graph) of the heat capacity at atmospheric pressure between the correlation Eq. (13), as well as the present and other calculated data [14–17]. Deviation statistics are summarized in Table 3.

Table 3. Summary of all the main isobaric data on the fish oil heat capacity, as well as their standard deviations (St.Err.), average absolute relative deviations (AAD) and maximum average absolute relative deviations (MAAD) with respect to Eq. (13) at atmospheric pressure

Authors	St.Err, %	AAD, %	MADD, %
Bondi [12]	1.94	6.36	4.17
Filipov [14]	2.22	2.6	3.86
Ruzicka [15]	16.49	23.1	15.15
Ceriani [16]	33.13	23.1	46.55
Xiaoyi Zhu [17]	13.14	24.3	16.41
This work	0.15	0.11	0.19

Based on the data (Fig. 8, Table 3), we can conclude that, for example, calculations using the method proposed by Ruzicka [15] demonstrated deviations from Eq. (13) of up to -15.15%. Such significant differences are probably associated with the size of the group component of double bonds. Calculation

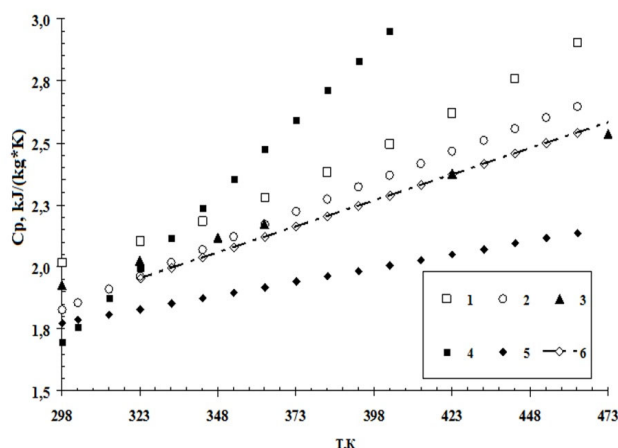


Fig. 7. Heat capacity of fish oil at atmospheric pressure: dotted line – calculation using Eq. (13); 1 – Ruzicka [15]; 2 – Bondi [12]; 3 – Filippov [14]; 4 – R. Ceriani [16]; 5 – Xiaoyi Zhu [17]; 6 – this work.

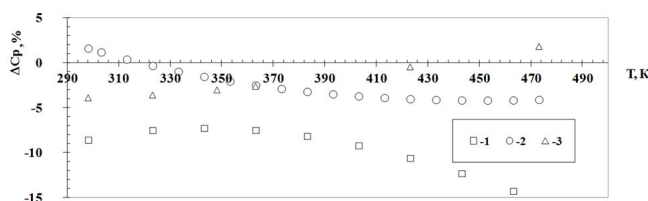


Fig. 8. Deviations $\Delta C_p = (C_{\text{experimental}} - C_{\text{calculated}})/C_{\text{experimental}} \cdot 100\%$ of all available data on the fish oil isobaric heat capacity from Eq. (13) depending on temperature at atmospheric pressure: 1 – Ruzicka [15]; 2 – Bondi [12]; 3 – Filippov [14].

using the method proposed by Filippov [14] showed deviations with increasing temperature ranging from -3.86 to $+1.87\%$. The calculation according to Bondi [12] demonstrated deviations from 1.6 to 4.2% . Significant deviations in the calculated values of Ceriani [16] up to 46% and Zhu [17] up to 16.5% are associated with the limited experimental data used in selecting the constants.

To assess the effect of pressure on the fish oil heat capacity and compare it with experimental data, the calculation equation proposed by Filippov [14] was used:

$$\frac{\Delta C_p}{R} = 7,77 - 10,33 \cdot \lg(A) + \frac{37(\chi - 0,17)}{1 - 1,45 \cdot \chi}, \quad (19)$$

where $\Delta C_p = C_p - C_p^0$; $\chi = \varphi - 0,31 \tau$; $\tau = T/T_{cr}$; $\varphi = V/V_{cr}$; C_p^0 – ideal gas heat capacity, calculated using the method of Rihany and Doraiswamy [13]; Filippov's criterion A was calculated based on the increments given in [14]. Critical parameters are determined by structural composition based on group components according to [12]. The results of comparison of heat capacity under pressure are shown in Fig. 9.

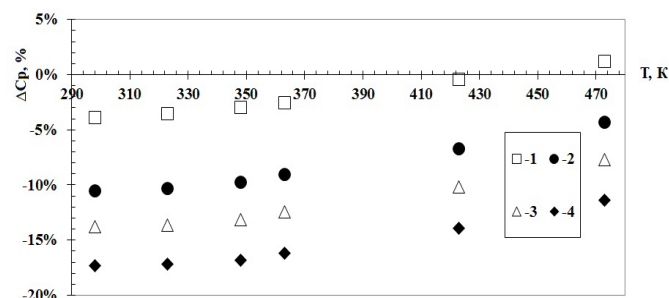


Fig. 9. Deviations $\Delta C_p = (C_{\text{experimental}} - C_{\text{calculated}})/C_{\text{experimental}} \cdot 100\%$ of calculated data on the fish oil isobaric heat capacity using Filippov's method from Eq. (13) depending on temperature at different pressures: 1 – 9.8 MPa; 2 – 19.6 MPa; 3 – 29.4 MPa; 4 – 39.2 MPa.

The average error in calculating the heat capacity of fish oil according to Eq. (19) at pressure $P = 0.098$ MPa in the temperature range from 323.15 to 423.15 K lies within $\pm 5\%$. At pressures above atmospheric, with pressure increasing to 39.2 MPa, the calculated data (Eq. (19)) are overestimated relative to Eq. (13) by 5 to 17% . This is much higher than the corresponding error estimate calculated using Eq. (15) [14]. Deviations of the calculated data of Filippov's Eq. (19) from the correlation Eq. (13) are associated with restrictions on χ .

5. Conclusion

Direct measurements of the isobaric heat capacity of a fish oil sample (OMEGA-3 "950") under pressure were carried out using a differential scanning calorimeter. New experimental data on heat capacity were obtained at pressures up to 39.2 MPa and temperatures up to 473.15 K, which significantly expands the temperature and pressure ranges of literature data on the isobaric heat capacity of a fish oil sample. A correlation equation has been developed that represents experimental data on the heat capacity of fish oil with an error of less than 0.3% in the studied range of temperatures and pressures.

Acknowledgments

The work was carried out with financial support from the Russian Science Foundation (project No. 23-79-10304, <https://rscf.ru/project/23-79-10304/>).

References

- [1]. J. Cvengroš, Z. Cvengrošová, *Biom. Bioener.* 27 (2004) 173–181. DOI: [10.1016/j.biombioe.2003.11.006](https://doi.org/10.1016/j.biombioe.2003.11.006)

- [2]. S.V. Mazanov, F.M. Gumerov, R.A. Usmanov, et al., Biodiesel fuel. Part I. Methods of obtaining. Power engineering: research, equipment, technology. 24 (2022) 16–49. (In Russ.). DOI: [10.30724/1998-9903-2022-24-4-16-49](https://doi.org/10.30724/1998-9903-2022-24-4-16-49)
- [3]. K. Iyer, P. Prasad, S. Mythili, A. Sathiavelu, *International Journal of Life Sciences and Technology* 4 (2011) 19–30. <https://www.proquest.com/docview/1221243324?sourcetype=Scholarly%20Journals>
- [4]. J. Ferrell, V. Sarisky-Reed. National Algal Biofuels Technology Roadmap: A technology roadmap resulting from the National Algal Biofuels Workshop and Roadmap sponsored by the U.S. Department of Energy Office of Energy Efficiency and Renewable Energy Office of the Biomass Program Publication Date: May 2010, p. 140. https://www1.eere.energy.gov/bioenergy/pdfs/algal_biofuels_roadmap.pdf
- [5]. N.M. Verma, S. Mehrotra, A. Shukla, B.N. Mishra, *Afr. J. Biotechnology* 9 (2010) 1402–1411. DOI: [10.5897/AJBx09.071L](https://doi.org/10.5897/AJBx09.071L)
- [6]. L. Gouveia, A.C. Oliveira, *J. Ind. Microbiol Biotechnol.* 36 (2009) 269–274. DOI: [10.1007/s10295-008-0495-6](https://doi.org/10.1007/s10295-008-0495-6)
- [7]. X. Li, J. Liu, G. Chen, et al., *Algal Research* 43 (2019) 101619. DOI: [10.1016/j.algal.2019.101619](https://doi.org/10.1016/j.algal.2019.101619)
- [8]. S. Sathivel, W. Prinyawiwatkul, I.I. Negulescu, et al, *J Am. Oil Chem. Soc.* 85 (2008) 291–296. DOI: [10.1007/s11746-007-1191-9](https://doi.org/10.1007/s11746-007-1191-9)
- [9]. S. Sathivel, *J. Am. Oil Chem. Soc.* 82 (2005) 147–157. DOI: [10.1007/s11746-005-1057-6](https://doi.org/10.1007/s11746-005-1057-6)
- [10]. F.N. Shamsetdinov, S.A. Bulaev, Z.I. Zari-pov, *Bulletin of Kazan State Technical University named after A.N. Tupolev* [Vestnik Kazanskogo gosudarstvennogo tehničeskogo universiteta im. A.N. Tupoleva] 2 (2011) 11–16. (in Russ.). https://www.elibrary.ru/download/elibrary_16458452_32724892.pdf
- [11]. Z.I. Zari-pov, S.V. Mazanov, J.M. Kouagou, et al., *Bulletin of Kazan State Technical University named after A.N. Tupolev* [Vestnik Kazanskogo gosudarstvennogo tehničeskogo universiteta im. A.N. Tupoleva] 4 (2021) 9–13. (in Russ.). <https://www.elibrary.ru/item.asp?id=48080563>
- [12]. A. Bondi, *Ind. Eng. Chem. Fundamen.* 5 (1966) 442–449. DOI: [10.1021/i160020a001](https://doi.org/10.1021/i160020a001)
- [13]. D.N. Rihani, L.K. Doraiswamy, *Ind. Eng. Chem. Fundamen.* 4 (1965) 17–21. DOI: [10.1021/i160013a003](https://doi.org/10.1021/i160013a003)
- [14]. L.P. Filippov. Prediction of thermophysical properties of liquids and gases [Prognozirovanie teplofizicheskikh svojstv zhidkostej i gazov]. M.: Energoatomizdat, 1988, 167 p. (in Russ.). ISBN: 5-283-00009-5
- [15]. V. Ruzicka, E.S. Domalski, *J. Phys. Chem. Ref. Data* 22 (1993) 619–657. DOI: [10.1063/1.555924](https://doi.org/10.1063/1.555924)
- [16]. R. Ceriani, R. Gani, A.J.A. Meirelles, *Fluid Phase Equilib.* 283 (2009) 49–55. DOI: [10.1016/j.fluid.2009.05.016](https://doi.org/10.1016/j.fluid.2009.05.016)
- [17]. X. Zhu, D.M. Phinney, S. Paluri, D.R. Heldman, *J. Food Sci.* 83 (2018). DOI: [10.1111/1750-3841.14089](https://doi.org/10.1111/1750-3841.14089)
- [18]. E.S. Platonov. Thermophysical measurements in monotonic mode [Teplofizicheskie izmerenija v monotonom rezhime]. L.: Energy, 1972, 143 p. (in Russ.).
- [19]. R.A. Usmanov, R.R. Gabitov, Sh.A. Biktashev, et al., *Russ. J. Phys. Chem.* 5 (2011) 1216–1227. DOI: [10.1134/S1990793111080112](https://doi.org/10.1134/S1990793111080112)
- [20]. Z.I. Zari-pov, A.U. Aetov, R.R. Nakipov, et al., *J. Molec. Liq.* 307 (2020) 112935. DOI: [10.1016/j.molliq.2020.112935](https://doi.org/10.1016/j.molliq.2020.112935)
- [21]. Z.I. Zari-pov, A.U. Aetov, R.R. Nakipov, et al, *J. Chem. Thermodyn.* 152 (2021) 106270. DOI: [10.1016/j.jct.2020.106270](https://doi.org/10.1016/j.jct.2020.106270)
- [22]. W. Wagner, A. Pruß, *J. Phys. Chem. Ref. Data* 31 (2002) 387–535. DOI: [10.1063/1.1461829](https://doi.org/10.1063/1.1461829)
- [23]. E.W. Lemmon, E.W. Bell, M.L. Huber, M.O. McLinden, 2018. NIST Standard Reference Database 23: Reference Fluid Thermodynamic and Transport Properties-REFPROP, Version 10.0.
- [24]. Z.I. Zari-pov, R.R. Nakipov, S.V. Mazanov, F.M. Gumerov, *Russ. J. Phys. Chem.* 98 (2024) 2256–2261. DOI: [10.1134/S0036024424701413](https://doi.org/10.1134/S0036024424701413)